



Rheological and Tribological Study of Polyethylsiloxane with SiO₂ Nanoparticles Additive

Tuyana Dembelova ^{1,2,*} , Badma Badmaev ¹, Dagzama Makarova ¹, Aleksandr Mashanov ¹
and Undrakh Mishigdorzhijn ¹

¹ Institute of Physical Materials Science of the Siberian Branch of the Russian Academy of Sciences, 670047 Ulan-Ude, Russia

² Laboratory of Physics of Disordered Systems, Banzarov Buryat State University, 670000 Ulan-Ude, Russia

* Correspondence: dembelova@ipms.bsnet.ru or tu_dembel@mail.ru

Abstract: Nowadays, much attention is paid to the creation of high-performance lubricants with improved properties through the use of ultrafine nanopowders. The paper shows the results of studying the viscoelastic properties of samples of silicon dioxide nanoparticle suspensions based on polyethylsiloxane (silicone oil) by the acoustic resonance method. The method is based on a study of the additional coupling effect on the resonance characteristics of the piezoelectric resonator. The values of the shear modulus and the tangent of the mechanical loss angle were calculated. The interaction between polymer molecules and nanoparticles was characterized by infrared spectroscopy. The influence of silicon dioxide nanoparticles (as a nano-additive) on the performance characteristics of polyethylsiloxane lubricant is presented. The results of determining the friction coefficient from the sliding speed show an increase in the tear strength of the lubricating film, leading to improved tribological properties.

Keywords: polyethylsiloxane; silicon dioxide nanoparticles; shear elasticity; mechanical loss tangent; lubricant additive; tribological performance



Citation: Dembelova, T.; Badmaev, B.; Makarova, D.; Mashanov, A.; Mishigdorzhijn, U. Rheological and Tribological Study of Polyethylsiloxane with SiO₂ Nanoparticles Additive. *Lubricants* **2023**, *11*, 9. <https://doi.org/10.3390/lubricants11010009>

Received: 30 November 2022

Revised: 19 December 2022

Accepted: 23 December 2022

Published: 26 December 2022



Copyright: © 2022 by the authors. Licensee MDPI, Basel, Switzerland. This article is an open access article distributed under the terms and conditions of the Creative Commons Attribution (CC BY) license (<https://creativecommons.org/licenses/by/4.0/>).

1. Introduction

One of the most effective methods to significantly improve the reliability and wear resistance of machines and mechanisms is to improve the quality of lubricants by introducing various additives into the base lubricants that improve the tribological properties of the lubricating medium.

The efficiency of nanomaterials and nanofunctional additives application is confirmed by numerous research results. The introduction of nanoparticles into the lubricating medium allows for increasing the resource of tribocouplings of supporting units of mechanisms and machines. In [1–10], the influence of nanoparticles on friction and wear was analyzed. Much attention is paid to methods for stabilizing nanoparticles in lubricants and their compatibility with base oil [1,3,8,9]. Characteristics of lubricants depend on the chemical nature of nanoparticles, their morphology, concentration, and size [1–3,7,10]. In [5,6,9], an analysis of worn friction surfaces after the application of nanolubricants was carried out, which shows the effectiveness of the use of nanoparticles. There are several types of friction and lubrication mechanisms involving nanoparticles [2–4,7–9], the main types of lubrication mechanisms include the ball-bearing effect, the formation of a protective film, the healing effect, and the polishing effect.

The addition of nanoparticles significantly changes the physical properties of liquids. Nanoparticles, as a dispersed phase, lead to the appearance of a volumetric spatial structural grid throughout the volume of the dispersed system. This changes the structural and mechanical properties of the disperse system and complicates the relaxation processes occurring in it [10–14]. Rheological properties that characterize these systems, such as

elastic modulus, viscosity, and strength depend on the concentration of nanoparticles, their size, the nature of the dispersed phase, and the dispersion medium. In this regard, it is important to study the features of viscoelastic parameters of the lubricant dispersions and study the influence of nano-additives on their performance properties. This paper presents the results of such research by the acoustic resonance method on the example of PES-2 silicone oil.

The selection of polyorganosiloxanes (silicone oils) as the base liquid is justified by their wide application in modern technology. The common properties of these polymeric liquids are high thermal stability, ample dielectric, hydrophobic properties, and low surface tension coefficient. Their viscosity weakly depends on temperature. A wide operating temperature range and sufficient lubricating properties allow their use as coolants, polishing agents, greases, instrument oils, and as hydraulic brake fluids. In a number of silicone oils, polyethylsiloxanes (PES) have excellent low-temperature properties due to their structure, so they are the basis for arctic freeze-resistant lubricants. Despite all the advantages, they have low values of intermolecular interaction forces, which are manifested in their mechanical properties. The low tear strength of polymer films does not allow their use for highly loaded friction units, such as wheel bearings. In the works [14–22], the problems of improving the rheological and tribological properties of polyorganosiloxanes by changing the molecular structure and selecting the optimal composition of greases based on them are discussed. The purpose of this work is to study the rheological properties of polyethylsiloxane oil with the addition of silicon dioxide nanoparticles, and the change in their tribological properties compared to the base oil, taking into account the interaction between the base oil and the nanoparticles.

2. Materials

In the present research, dispersions of silicon dioxide nanoparticles are studied, where polyethylsiloxane liquid is used as a base liquid. PES-2 polyethylsiloxane liquid, which meets the requirements of GOST 13004-77, is used [23]. PES-2 is a mixture of polymers of linear $(C_2H_5)_3Si-O-[Si(C_2H_5)_2O]_3-Si(C_2H_5)_3$ and cyclic $[(C_2H_5)_2SiO]_3$ structures or linear polymers. Table 1 shows the main properties of the polyethylsiloxane liquid PES-2 [15].

Table 1. Main characteristics of polyethylsiloxane liquid PES-2 [15].

Molecular Weight	Density 20 °C, kg/m ³	Viscosity, mm ² s ⁻¹			Boiling Point, °C (133–400 Pa)	Pour Point, °C
		−60 °C	20 °C	60 °C		
341	940	312	9	4	110–150	−110

Silicon dioxide SiO₂ nanopowders of the Tarkosil trademark with dimensions of 100 nm, 50 nm (T-05) and 20 nm (T-20) are used to prepare samples of nanoparticle dispersions. Silicon dioxide nanoparticles are characterized by the presence on the surface of OH groups with a concentration in the range of $(0.5 \div 4)/nm^2$, depending on the characteristics of the production method [24]. The properties of dispersed systems depend on the degree of dispersion of nano-inclusions. Nanoparticles have high surface energy and form agglomerates of up to a few micrometers in the disperse medium. Figure 1 shows SEM images of the powders obtained using a JEOL JSM-6510LV SEM. It can be seen that as the specific surface area of the particles increases, the sizes of the agglomerates grow, significantly exceeding the primary sizes of the silicon dioxide particles. In order to obtain a stable suspension, it is important to disperse it thoroughly, which allows maximum destruction of agglomerates of nanoparticles. In addition, dispersing establishes a uniform distribution of nanoparticles in the volume. Our suspensions are produced by the ultrasonic method; the optimal dispersing time of 30 min for SiO₂/PES-2 has been determined experimentally. The average T-05 particles size in the suspension measured by the Nano Particle Size Analyzer SALD-7500nano is 78 nm [25].

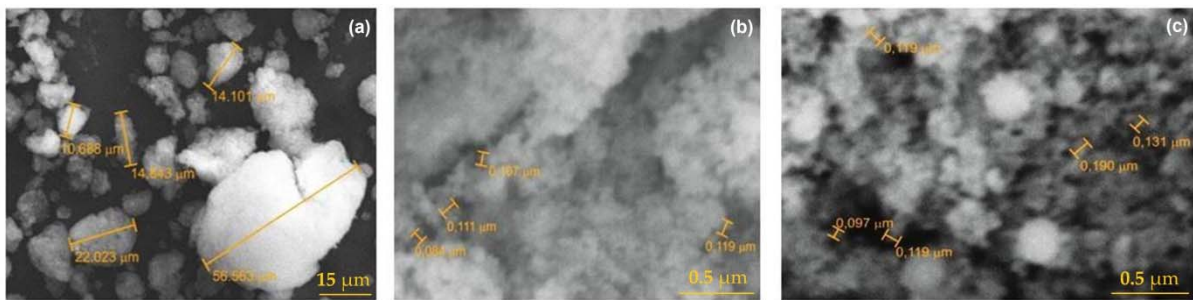


Figure 1. Electronic photograph of silicon dioxide nanoparticles SiO_2 : (a) T-20 (20 nm); (b) T-05 (50 nm); (c) SiO_2 (100 nm) [25].

3. Methods

In the study of the relaxation properties of liquid condensed media, it is convenient to use dynamic methods, for example, when the liquid is subjected to cyclic deformation-shear action with a certain frequency. An acoustic resonance method with a piezoquartz resonator was used in the work. It allows liquids with a wide viscosity range from 10^{-3} to 10^5 Pa·s to be investigated and is successfully used to study the shear dynamic properties of colloidal dispersions of nanoparticles of different viscosities. The method is applicable to the study of liquid interlayers within a wide range (1–100 μm) of thickness.

The resonance method is based on the study of the influence of additional coupling forces on the resonance characteristics of an oscillating system [26,27]. A piezoquartz crystal fixed by two steel needles at points on the nodal line oscillates at the basic resonant frequency. Liquid is applied to one end of the horizontal surface of the piezoquartz, making tangential displacements and covered with a plate of fused quartz, Figure 2. The piezoquartz cut of $X-18.5^\circ$ provides pure shear deformations of the liquid and standing shear waves are established in it. The solution of the interaction problem of the resonator with the liquid layer and the solid cover-plate gives for the complex shift of resonant frequency $\Delta\omega$ the following expression:

$$\Delta\omega = \frac{2SG * \kappa}{M\omega} \cdot \frac{1 + \cos(2\kappa H - \varphi)}{\sin(2\kappa H - \varphi)}, \quad (1)$$

where $G^* = G' + iG''$ is the complex shear modulus of the liquid, G' -elastic part of the modulus (the storage modulus), G'' -viscous part of the modulus (the loss modulus), S is the contact area of the liquid with the piezoquartz, H is the thickness of the interlayer, M is the mass of the piezoquartz, $\varphi = \varphi' + i\varphi''$ is the complex phase shift upon reflection of the shear wave from the liquid-plate interface, $\kappa = \beta - i\alpha$ is the complex wave number of the liquid.

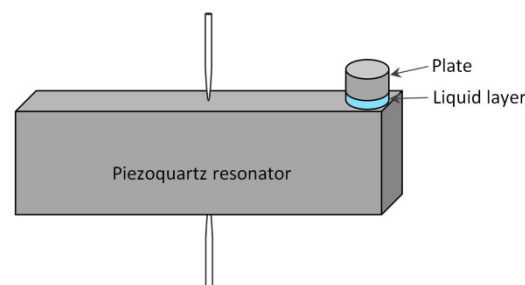


Figure 2. Piezoquartz resonator with additional coupling.

When the piezoelectric quartz vibrates, the plate, which has sufficient mass, practically rests due to the weak connection carried out by the liquid layer, therefore $\varphi = 0^\circ$. Division

of the complex shift of the piezoquartz resonant frequency into real and imaginary parts gives the following equations for the linear frequency:

$$\Delta f' = \frac{SG'\beta}{4\pi^2 M f_0 \cos \theta} \cdot \frac{\sin 2\beta H - \tan^{\theta/2} \sinh(2\beta H \cdot \tan^{\theta/2})}{\cosh(2\beta H \cdot \tan^{\theta/2}) - \cos 2\beta H}, \quad (2)$$

$$\Delta f'' = \frac{SG'\beta}{4\pi^2 M f_0 \cos \theta} \cdot \frac{\sin 2\beta H \cdot \tan^{\theta/2} + \sinh(2\beta H \cdot \tan^{\theta/2})}{\cosh(2\beta H \cdot \tan^{\theta/2}) - \cos 2\beta H}, \quad (3)$$

where f_0 is the natural resonance frequency of the piezoquartz. $\tan(\theta/2) = \alpha/\beta$, where β and α are the real and imaginary parts of the wave number κ . These equations show that, given liquid properties, the real and imaginary frequency shifts are functions of the film thickness. With an increase in the latter, damp oscillations of the frequency shifts should be observed. According to the theory of the method, the shear wavelength λ can be determined from the maximum attenuation [26–29]. By equating the thickness derivative of the imaginary frequency shift (3) to zero we obtain the positions of the maximum attenuation values. The first damping maximum will be observed when the thickness of layer H is equal to $\lambda/2$. The dynamic modulus of the shear elasticity of a liquid with density ρ is determined by the equation:

$$G' = \lambda^2 f_0^2 \rho \cos \theta \cos^2 \frac{\theta}{2}. \quad (4)$$

In the case of a small thickness of the liquid layer, when $H \ll \lambda$, the following calculation formulas for the real and imaginary parts of the complex shear modulus come out from Equations (2) and (3):

$$G' = \frac{4\pi^2 M f_0 \Delta f' H}{S}, G'' = \frac{4\pi^2 M f_0 \Delta f'' H}{S} \quad (5)$$

It follows that in the presence of liquid shear modulus, the real $\Delta f'$ and imaginary $\Delta f''$ shifts of the resonant frequency should be proportional to the inverse value of the thickness of the liquid layer. The imaginary shift of the resonant frequency is determined by the change in the damping of the oscillating system. The tangent of the mechanical loss angle, which characterizes the energy loss, will be equal to:

$$\tan \theta = \frac{\Delta f''}{\Delta f'} \quad (6)$$

θ is the phase shift between the applied stress and strain, so the greater the dissipative losses, the greater θ . The maximum energy losses corresponding to the maximum G'' occur when the time of the force action coincides in magnitude with the relaxation time τ .

Thus, to determine the complex shear modulus of liquids at the small thickness of the liquid layer, it is sufficient to determine the dependencies of the real and imaginary shifts of the resonant frequency on the inverse value of the thickness of the liquid layer. Thickness of the liquid interlayer was measured by the optical method. A piezoquartz resonator with dimensions of 34.9 mm × 12 mm × 6 mm and mass $M = 6.82$ g, the basic resonant frequency $f_0 = 73.2$ kHz is used in the work. Base area of the plate is $S = 0.2$ cm². The conducted earlier studies have shown that a thorough cleaning of the working surfaces, proving sufficient wetting, is of particular importance for the reproducibility of measurement results [29].

The proposed method is not inferior to the world-famous methods used to study the viscoelastic properties of liquids, in particular, applied to low frequencies. Studies of pure liquids using this method at a frequency of about 10⁵ Hz have shown that there is a low-frequency viscoelastic relaxation in low-viscosity liquids [26,30,31]. It is known that the high-frequency relaxation process in liquids, observed at shear frequencies of 10¹⁰–10¹² Hz, is explained by the nature of the diffusion mobility of individual particles in a liquid [32]. Apparently, low-frequency viscoelastic relaxation is due to the collective

interaction of large groups of molecules. Therefore, the relaxation time can be many orders of magnitude longer than the settling time of individual liquid molecules. Low-frequency viscoelastic relaxation in liquids is confirmed in works [33–36], devoted to the detection of the solid-like properties of liquids away from phase transitions.

4. Results and Discussion

Figure 3 shows the experimental results of measuring $\Delta f'$ -real and $\Delta f''$ -imaginary frequency shifts depending on the inverse of the liquid layer thickness for the sample of a colloidal suspension of SiO₂ nanoparticles in polyethylsiloxane liquid PES-2 with a concentration of $c = 1.25$ wt.% and particle size $d = 50$ nm at room temperature. It can be seen from the figure that the dependences of the real and imaginary frequency shifts on the inverse layer thickness $1/H$ are linear. According to the formulas (5), this indicates that this suspension has a measurable shear modulus in this suspension does not depend on the layer thickness. Extrapolation of linear dependences shows that they tend to the origin of coordinates. Calculations using the formulas of the method (5), (6) gives values for the dynamic shear modulus of $0.23 \cdot 10^5$ Pa, and for the tangent of the mechanical loss angle of 0.21.

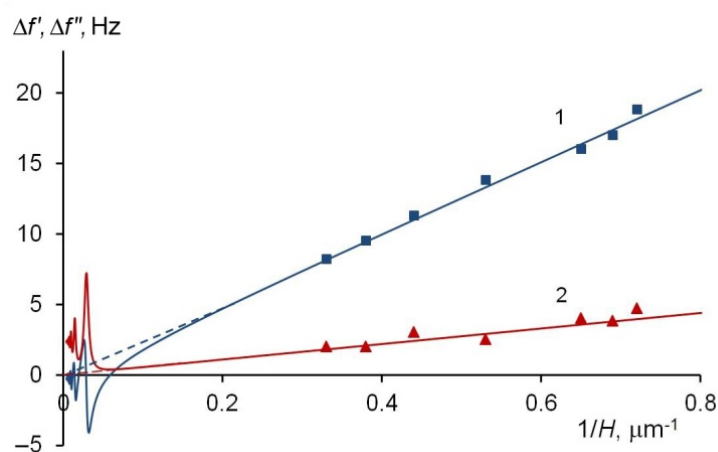


Figure 3. Theoretical (blue and red curves) and experimental (points) dependences of the real (1) and imaginary (2) shifts of the resonant frequency of the piezoquartz on the inverse thickness of the SiO₂/PES-2 suspension interlayer, $c = 1.25$ wt.%, $d = 50$ nm.

The solid lines in Figure 3 show the theoretical dependences of the real and imaginary shifts of the resonant frequency, calculated for these values of G' and $\tan\theta$ by Equations (2) and (3). The figure shows agreement between the experimental points and theoretical curves. With an increase in the thickness of the interlayer, frequency shift oscillations are observed in accordance with the theory of the method.

The dependence of viscoelastic properties on the size of nanoparticles can be traced by examining SiO₂/PES-2 suspensions with the same concentration of nanoparticles. Table 2 presents the values of the real shear modulus G' , the tangent of the mechanical loss angle $\tan\theta$ for suspensions of silicon dioxide nanoparticles of different diameters d in PES-2 polyethylsiloxane liquid with the concentration of particles $c = 0.5$ wt.% at a temperature of 23 °C. The table shows that the elastic modulus of suspensions grows with increasing particle diameter. The tangent of the mechanical loss angle decreases, while remaining less than unity. The last column shows values of the relaxation frequency $f_{\text{rel}} = f_0 \cdot \tan\theta$, calculated according to the mechanism of Maxwell's stress relaxation. It can be seen that the obtained values of f_{rel} for SiO₂/PES-2 are less than the frequency of shear vibrations realized in the experiment.

Table 2. Viscoelastic characteristics of suspensions of SiO₂/PES-2 nanoparticles.

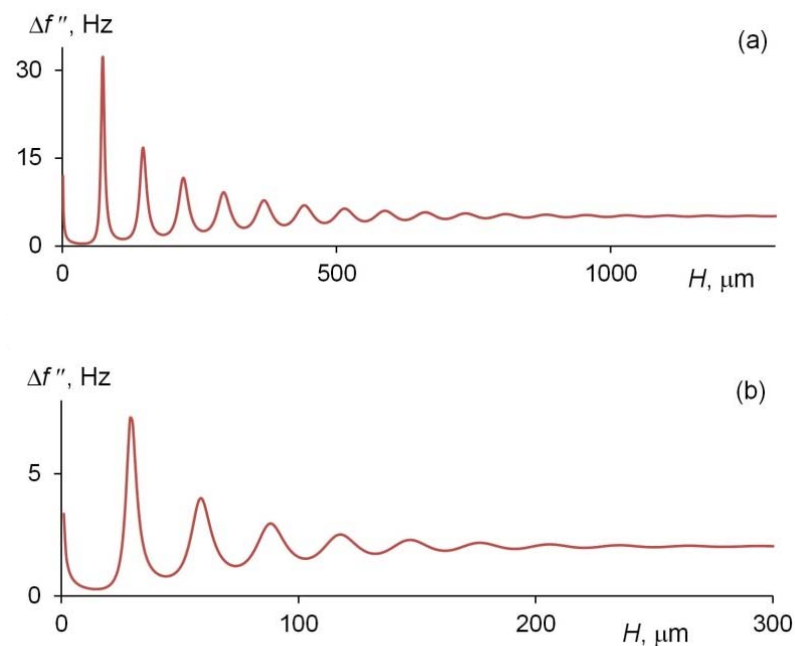
Dispersion	d , nm	t , °C	c , wt.%	$G' \cdot 10^{-5}$, Pa [37]	$\tan\theta$ [37]	f_{rel} , kHz
SiO ₂ /PES-2	20	23	0.5	0.09	0.73	53.43
	50	23	0.5	0.17	0.18	13.18
	100	23	0.5	1.08	0.10	7.32

It is well known that viscous waves in liquid are rapidly damped. The penetration depth of shear wave δ or the distance at which the wave amplitude decreases by a factor of e depends on the value of θ [38]:

$$\delta = \frac{\lambda}{2\pi \tan \theta/2}. \quad (7)$$

For a Newtonian fluid, viscous waves are almost completely attenuated at a distance of one wavelength. If the liquid exhibits viscoelastic properties at a given frequency of shear deformations and $\tan\theta < 1$, the shear wave penetration depth may be quite large. The works of [26–29,37,39,40] determined experimentally the shear moduli from the propagation of low-frequency shear waves in polymeric liquids at a shear vibration frequency of the order of 10^5 Hz and showed satisfactory agreement between the results obtained by formulas (4) and (5). These works indicate that low-frequency shear elasticity is a property of the fluid in the volume and does not refer to boundary phenomena.

Figure 4 shows the theoretical dependences of $\Delta f''(H)$ for the studied SiO₂/PES-2 suspensions calculated by formula (3) using the data in Table 2. As the thickness of the liquid layer increases, the imaginary frequency shift tends to the limiting value $\Delta f''$. With thickness, the frequency shift oscillations gradually disappear. For a suspension with nanoparticles size of $d = 100$ nm and $\tan\theta = 0.1$, the values of $\Delta f''_{max}$ and $\Delta f''_{min}$ are equal to within 1% at the liquid layer thickness of $H \approx 1.3$ mm, and the piezoelectric stops detecting the influence of reverse wave. As $\tan\theta$ increases, the depth of wave penetration decreases. Thus, for suspensions with a particle diameter of $d = 50$ nm and 20 nm, the $\Delta f''$ oscillations disappear when the suspension interlayer thickness is ~ 300 μm and ~ 90 μm (Figure 4b,c).

**Figure 4.** Cont.

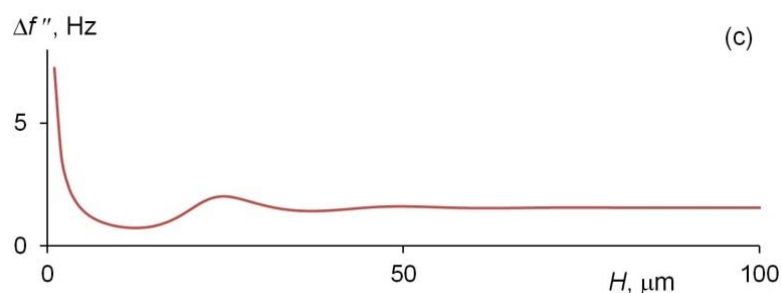


Figure 4. Theoretical curves of the dependence of the imaginary shift of the resonant frequency on the layer thickness of suspension of nanoparticles SiO₂/PES-2, $c = 0.5$ wt.%. (a) $d = 100$ nm; (b) $d = 50$ nm; (c) $d = 20$ nm.

The presented studies of the viscoelastic properties of SiO₂/PES-2 suspensions were carried out at small angles of shear deformation of no more than 10' in the region of linear elasticity, where the shear modulus has a constant value. It can be assumed that the equilibrium supramolecular structure of the liquid with a relatively long relaxation period and finite strength is preserved in this region. The supramolecular structure can be due to the bonds formed during the interaction of the polymer with nanoparticles. As shown in our previous works [25,41], the shear modulus G' decreases with an increase in the shear strain angle at a certain critical value of the shear stress, and the mechanical loss tangent increases due to the destruction of the supramolecular structure of the liquid and changes in its viscoelastic properties. The peculiarities of the relaxation properties of silicone oils and data on the shear wave penetration depth in viscoelastic fluids make it possible to consider the effect of shear elasticity on their performance characteristics in various applications, including tribology [21,25,42,43].

Infrared spectra of the studied samples were obtained to characterize the interaction between the dispersion medium and the dispersed phase. Spectrometric studies of the functional groups of the studied dispersions were carried out on an ALPHA IR-Fourier spectrometer (Bruker, Leipzig, Germany) by the attenuated total reflectance (ATR) method. In the IR spectrum of silicon dioxide particles with sizes of 100 and 50 nm, distinctive absorption peaks of siloxane and silanol groups were found [25], which can be explained by the presence of OH groups on the particle surface.

Changes in the infrared spectra of the SiO₂/PES-2 dispersions in comparison with the spectrum of the PES-2 base liquid may indicate the nature of the interaction of the polyethylsiloxane liquid with nanoparticles. Figure 5 shows the IR spectra for PES-2 and suspensions of silicon dioxide nanoparticles with concentrations of $c = 0.5$ and $c = 1.25$ wt.% and a diameter of $d = 50$ nm. There is a shift of the band maximum at 1060.48 cm⁻¹, corresponding to the stretching vibration of the Si–O bond, to 1062.52 cm⁻¹, indicating the strengthening of this bond. Along with this, the energy of the Si–C valence bond increases with a shift in the position of the maximum from 689.311 to 691.351 cm⁻¹. For suspension with a higher concentration $c = 1.25$ wt.%, a shift in the absorption band of the C–H valence bond from 2912.24 to 2914.28 cm⁻¹ is observed. Such small shifts are related to the small concentrations of nanoparticles in the suspension. By subtracting the IR spectrum of PES-2 from the spectrum of suspensions with particle concentrations of 1.25 and 5 wt.%, broad absorption bands were obtained in the frequency range of 3675 cm⁻¹ [25], indicating the formation of hydrogen bonds between polyethylsiloxane molecules and silicon dioxide particles. It was found that with an increase in the concentration of nanoparticles in the suspension, the bands are more pronounced.

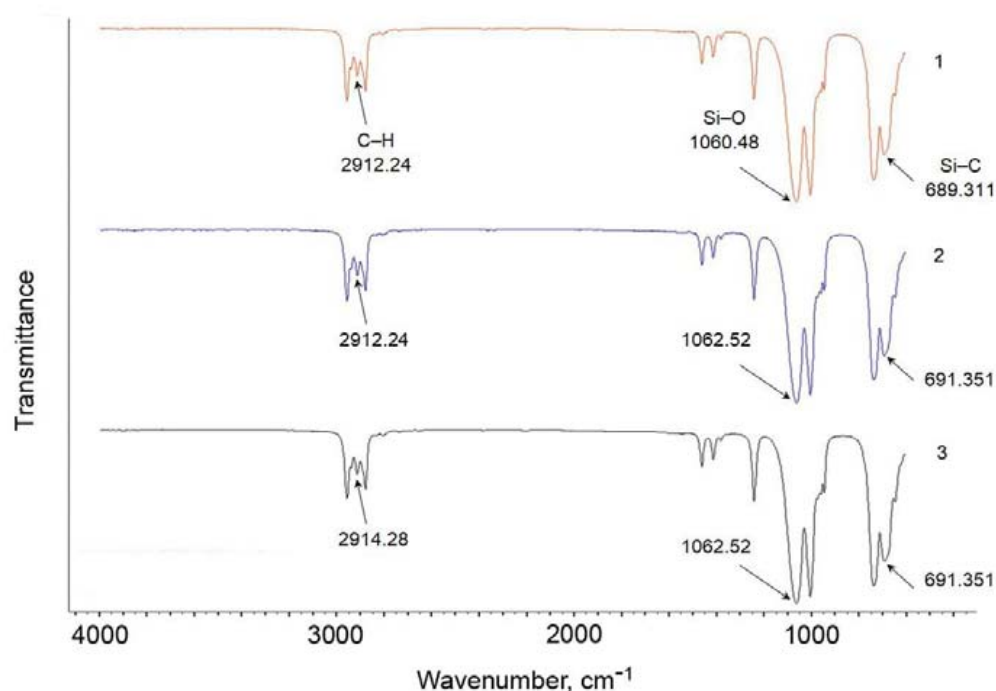


Figure 5. IR spectra: (1) PES-2; (2) SiO₂/PES-2, d = 50 nm, c = 0.5 wt%; (3) SiO₂/PES-2, d = 50 nm, c = 1.25 wt.%.

Based on the analysis of the obtained spectra, it can be concluded that the interaction of silicon dioxide nanoparticles with the polymer is caused by hydrogen bonds between hydroxyl groups on the surface of silicon dioxide with oxygen atoms in the polymer molecule, as well as possibly with a small number of alkyl groups in polymer chains. This contributes to the formation of a stronger suspension structure compared to the base liquid. It is known that silica fillers are used to improve the mechanical properties of polymeric materials and rubbers. For example, the tensile strength, modulus of elasticity, and elongation of polypropylene/low-density polyethylene nanocomposites can be simultaneously significantly improved by adding an optimal dosage of filler masterbatch containing in its composition 5 nm nano-silicon dioxides [44]. It was shown in [45,46] that the formation of a network due to hydrogen bonds between silica fillers and the matrix polymer can increase the tensile strength of siloxane polymers by several tens of times.

Polyethylsiloxanes are mainly used as lubricating oils in instruments and are a dispersion medium for low-temperature lubricants, ensuring the stable operation of instruments and mechanisms in the harsh conditions of the Arctic. This determines the interest in studying their tribological properties at low temperatures. The friction coefficient of a steel-steel pair with polyethylsiloxane lubricant was determined at $-25\text{ }^{\circ}\text{C}$ using a tribology device operating on the principle of a ball-on-3-plates attached to a Physica MCR 302 Rheometer (Anton Paar, Graz, Austria). The system has fast and accurate normal force control and a wide range of speed and torque. Temperature control is carried out by Peltier elements. The ball is pressed against the plates with the same load at all contact points and is driven into rotation by the rheometer drive. The coefficient of friction is calculated as the ratio of the friction force to the normal load. Figure 6 shows the dependence of the friction coefficient on the sliding speed when PES-2 and samples of dispersions of 50 nm SiO₂ nanoparticles in PES-2 were used as lubricants [42]. The normal load was of 5 N.

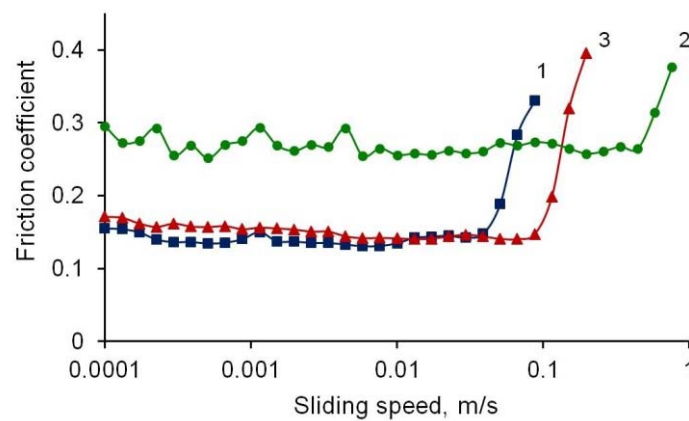


Figure 6. Dependence of the coefficient of friction of a steel–steel pair on the sliding speed ($t = -25\text{ }^{\circ}\text{C}$) with a lubricant: (1) PES-2; (2) SiO₂/PES-2, $c = 0.5\text{ wt } \%$, $d = 50\text{ nm}$; (3) SiO₂/PES-2, $c = 1.25\text{ wt } \%$, $d = 50\text{ nm}$.

From the curves of the dependences obtained, the critical sliding speed, at which the friction coefficient increases sharply, is revealed, obviously due to the destruction of the lubricating layer separating the rubbing surfaces. Figure 5 shows that the destruction of the layer of the lubricant modified by nanoparticles occurs at high speeds compared to the basic lubricant. It should be noted that at a lower concentration of nanoparticles, the critical speed is higher, but the friction coefficient increases. A similar observation was obtained when studying the dynamic properties of polydimethylsiloxane with silicon dioxide nanoparticles [45]. As the silica nanoparticle concentration decreases, the span of the linear viscoelasticity region, where G^* is constant with the increasing strain amplitude, increases. Then the shear modulus decreases with a further increase in the strain amplitude. The difference in the values of the friction coefficient is possibly due to the implementation of different lubrication mechanisms. To elucidate the features of the lubrication mechanism using oil modified with nano-additives, further rheological studies of suspensions with an extended range of nanoparticle concentrations by acoustic methods depending on the amplitude of shear deformation, as well as an analysis of worn surfaces after friction test, are required. The optimal combination of the concentration and size of nanoparticles in the base oil may allow a simultaneous improvement in the anti-friction and anti-seize properties of the lubricant.

Thus, it can be concluded that the addition of silicon dioxide nanoparticles to silicone oil leads to the tear strengthening of the lubricant, contributing to the improvement of antiseize and antiwear properties, which may lead to an increase in their carrying capacity. Varying the concentration and size of nano-additives in the base fluid will provide optimal parameters for the development of high-performance lubricants.

5. Conclusions

Polyorganosiloxanes have weak intermolecular interaction and high flexibility of the polymeric siloxane chain, as a result of which they have specific mechanical and rheological properties. This is the reason for their wide application use in modern engineering. However, they are characterized by low mechanical strength. The inclusion of silicon dioxide nanoparticles in the polyethylsiloxane oil can contribute to strengthening its structure, based on the interaction of SiO₂ nanoparticles with polymer molecules. This will improve the tribological characteristics of polyethylsiloxane oils by increasing the strength of the lubricating film. The obtained data on the rheological properties of dispersions of SiO₂ nanoparticles based on the PES-2 polymer liquid by the acoustic method will contribute to the solution of the fundamental problem of physical materials science related to the creation of new promising materials with the desired properties for various applications.

Author Contributions: Conceptualization, T.D. and B.B.; methodology, B.B., T.D. and D.M.; validation, D.M., T.D. and B.B.; formal analysis, T.D. and D.M.; investigation, T.D., D.M., A.M. and U.M.; resources, B.B.; writing—original draft preparation, T.D.; writing—review and editing, T.D., B.B. and U.M.; supervision, B.B.; project administration, T.D.; funding acquisition, B.B. All authors have read and agreed to the published version of the manuscript.

Funding: The work was performed under the IPMS SB RAS state budget project 0270-2021-0007.

Data Availability Statement: The data presented in this study are available on request from the corresponding author.

Conflicts of Interest: The authors declare no conflict of interest.

References

1. Oganeseva, E.Y.; Lyadov, A.S.; Parenago, O.P. Nanosized Additives to Lubricating Materials. *Russ. J. Appl. Chem.* **2018**, *91*, 1559–1573. [CrossRef]
2. Dai, W.; Kheireddin, B.; Gao, H.; Liang, H. Roles of nanoparticles in oil lubrication. *Tribol. Int.* **2016**, *102*, 88–98. [CrossRef]
3. Gulzar, M.; Masjuki, H.H.; Kalam, M.A.; Varman, M.; Zulkifli, N.W.M.; Mufti, R.A.; Zahid, R. Tribological performance of nanoparticles as lubricating oil additives. *J. Nanopart. Res.* **2016**, *18*, 223. [CrossRef]
4. Luo, T.; Wei, X.; Huang, X.; Huang, L.; Yang, F. Tribological properties of Al₂O₃ nanoparticles as lubricating oil additives. *Ceram. Int.* **2014**, *40*, 7143–7149. [CrossRef]
5. Wang, Y.; Zhang, L.; Liu, A.; Wu, C.; Li, W. Tribological performance of silicone oil based Al₂O₃ nano lubricant for an Mg alloy subjected to sliding at elevated temperatures. *Tribol. Int.* **2022**, *175*, 107779. [CrossRef]
6. Rawat, S.S.; Harsha, A.P.; Deepak, A.P. Tribological performance of paraffin grease with silica nanoparticles as an additive. *Appl. Nanosci.* **2018**, *9*, 305–315. [CrossRef]
7. Chen, H.; Zhang, L.; Li, M.; Xie, G. Synthesis of Core–Shell Micro/Nanoparticles and Their Tribological Application: A Review. *Materials* **2020**, *13*, 4590. [CrossRef]
8. Qu, M.; Yao, Y.; He, J.; Ma, X.; Feng, J.; Liu, S.; Hou, L.; Liu, X. Tribological study of polytetrafluoroethylene lubricant additives filled with Cu microparticles or SiO₂ nanoparticles. *Tribol. Int.* **2017**, *110*, 57–65. [CrossRef]
9. Peng, D.; Kang, Y.; Hwang, R.; Shyr, S.; Chang, Y. Tribological properties of diamond and SiO₂ nanoparticles added in paraffin. *Tribol. Int.* **2009**, *42*, 911–917. [CrossRef]
10. Ur'ev, N.B.; Emel'yanov, S.V.; Titov, K.A. Structure-rheological properties of oil suspensions based on technical carbon and nanoscale fillers. *Prot. Met. Phys. Chem. Surfaces* **2015**, *51*, 226–229. [CrossRef]
11. Minakov, A.; Rudyak, V.; Pryazhnikov, M. Rheological behavior of water and ethylene glycol based nanofluids containing oxide nanoparticles. *Colloids Surfaces A Physicochem. Eng. Asp.* **2018**, *554*, 279–285. [CrossRef]
12. Koppula, S.B.; Sudheer, N.V.V.S. A review on effect of adding additives and nano additives on thermal properties of gear box lubricants. *Int. J. Appl. Eng. Res.* **2016**, *11*, 3509–3526. [CrossRef]
13. Rudyak, V.Y.; Dimov, S.V.; Kuznetsov, V.V. On the dependence of the viscosity coefficient of nanofluids on particle size and temperature. *Tech. Phys. Lett.* **2013**, *39*, 779–782. [CrossRef]
14. Zolper, T.J.; Seyam, A.M.; Chen, C.; Jungk, M.; Stammer, A.; Stoegbauer, H.; Marks, T.J.; Chung, Y.-W.; Wang, Q. Energy Efficient Siloxane Lubricants Utilizing Temporary Shear-Thinning. *Tribol. Lett.* **2013**, *49*, 525–538. [CrossRef]
15. Sobolevsky, M.V.; Muzovskaya, O.A.; Popeleva, G.S. *Properties and Applications of Organosilicone Products*; Khimiya: Moscow, Russia, 1975; pp. 88–110.
16. Anisimov, A.A.; Visochinskaya, Y.S.; Buzin, M.I.; Vasil'ev, V.G.; Nikiforova, G.G.; Peregudov, A.S.; Dubovik, A.S.; Orlov, V.N.; Shchegolikhina, O.I.; Muzafarov, A.M. New polydimethylsiloxanes with bulky end groups: Synthesis and properties. *Bull. Acad. Sci. USSR Div. Chem. Sci.* **2019**, *68*, 1275–1281. [CrossRef]
17. Zolper, T.; Li, Z.; Chen, C.; Jungk, M.; Marks, T.; Chung, Y.-W.; Wang, Q. Lubrication Properties of Polyalphaolefin and Polysiloxane Lubricants: Molecular Structure–Tribology Relationships. *Tribol. Lett.* **2012**, *48*, 355–365. [CrossRef]
18. Zhiheng, W.; Dehua, T.; Xuejin, S.; Xiaoyang, C. Study on a new type of lubricating oil for miniature bearing operating at ultra-low temperature. *China Pet. Process. Petrochem. Technol.* **2018**, *20*, 93–100. Available online: <http://www.chinarefining.com/EN/Y2018/V20/I1/93> (accessed on 21 November 2022).
19. Chichester, C.W.; Nevskaya, A. Modeling Molecular Structure to Tribological Performance. 2016. Available online: <https://saemobilus.sae.org/content/2016-01-0291/> (accessed on 21 November 2022).
20. Chichester, C.W. Development of High Service Temperature Fluids. 2016. Available online: <https://saemobilus.sae.org/content/2016-01-0484/> (accessed on 21 November 2022).
21. Wu, W.; Li, P.; Wang, X.; Zhang, B. Grafting of thermotropic fluorinated mesogens on polysiloxane to improve the processability of linear low-density polyethylene. *RSC Adv.* **2022**, *12*, 12463–12470. [CrossRef]
22. Guan, X.; Cao, B.; Cai, J.; Ye, Z.; Lu, X.; Huang, H.; Liu, S.; Zhao, J. Design and Synthesis of Polysiloxane Based Side Chain Liquid Crystal Polymer for Improving the Processability and Toughness of Magnesium Hydrate/Linear Low-Density Polyethylene Composites. *Polymers* **2020**, *12*, 911. [CrossRef]

23. STAR. Available online: <https://star-pro.ru/gost/13004-77> (accessed on 28 November 2022).
24. Bardakhanov, S.P.; Vikulina, L.S.; Lysenko, V.I.; Nomoev, A.V.; Poluyanov, S.A.; Tuzikov, F.V. Analysis of Nanopowders by Small-Angle X-Ray Scattering Method's. *Sib. J. Phys.* **2012**, *7*, 107–116. [[CrossRef](#)]
25. Dembelova, T.S.; Balzhinov, S.A.; Makarova, D.N.; Vershinina, Y.D.; Bazarova, S.B.; Badmaev, B.B. Dynamic viscosity of dispersion of silica dioxide nanoparticles. *IOP Conf. Series Mater. Sci. Eng.* **2020**, *1000*, 012005. [[CrossRef](#)]
26. Badmaev, B.B.; Dembelova, T.S.; Damdinov, B.B. *Viscoelastic Properties of Polymer Liquids*; Buryat Scientific Center, SB RAS: Ulan-Ude, Russia, 2013; pp. 56–136.
27. Badmaev, B.B.; Dembelova, T.S.; Makarova, D.N.; Gulgenov, C.Z. Ultrasonic Interferometer on Shear Waves in Liquids. *Sov. Phys. J.* **2020**, *62*, 1708–1715. [[CrossRef](#)]
28. Badmaev, B.; Bazarov, U.; Derjaguin, B.; Budaev, O. Measurement of the shear elasticity of polymethylsiloxane liquids. *Phys. B+C* **1983**, *122*, 241–245. [[CrossRef](#)]
29. Badmaev, B.; Dembelova, T.; Damdinov, B.; Makarova, D.; Budaev, O. Influence of surface wettability on the accuracy of measurement of fluid shear modulus. *Colloids Surfaces A Physicochem. Eng. Asp.* **2011**, *383*, 90–94. [[CrossRef](#)]
30. Badmaev, B.B.; Damdinov, B.B.; Dembelova, T.S. Viscoelastic relaxation in fluids. *Bull. Russ. Acad. Sci. Phys.* **2015**, *79*, 1301–1305. [[CrossRef](#)]
31. Derjaguin, B.; Bazarov, U.; Zandanova, K.; Budaev, O. The complex shear modulus of polymeric and small-molecule liquids. *Polymer* **1989**, *30*, 97–103. [[CrossRef](#)]
32. Frenkel, J.I. *Kinetic Theory of Liquids*; Academy of Sciences of USSR: Moscow/Leningrad, Russia, 1959; pp. 195–248.
33. Collin, D.; Martinoty, P. Dynamic macroscopic heterogeneities in a flexible linear polymer melt. *Phys. A Stat. Mech. Appl.* **2003**, *320*, 235–248. [[CrossRef](#)]
34. Noirez, L.; Baroni, P. Identification of a low-frequency elastic behaviour in liquid water. *J. Phys. Condens. Matter* **2012**, *24*, 372101. [[CrossRef](#)]
35. Noirez, L.; Baroni, P. Identification of thermal shear bands in a low molecular weight polymer melt under oscillatory strain field. *Colloid Polym. Sci.* **2018**, *296*, 713–720. [[CrossRef](#)]
36. Zaccone, A.; Trachenko, K. Explaining the low-frequency shear elasticity of confined liquids. *Proc. Natl. Acad. Sci. USA* **2020**, *117*, 19653–19655. [[CrossRef](#)]
37. Makarova, D.N.; Dembelova, T.S.; Badmaev, B.B. Low-Frequency Shear Elasticity of a Colloid Nanosuspension. *Acoust. Phys.* **2020**, *66*, 613–615. [[CrossRef](#)]
38. Philippoff, W. Relaxation in polymer solutions, polymer liquids and gels. In *Physical Acoustics. Properties of Polymers and Nonlinear Acoustics*; Part B.; Mason, W.P., Ed.; Mir: Moscow, Russia, 1969; Volume II, pp. 9–109.
39. Badmaev, B.B.; Budaev, O.R.; Dembelova, T.S.; Damdinov, B.B. Shear elasticity of fluids at low-frequent shear influence. *Ultrasonics* **2006**, *44*, e1491–e1494. [[CrossRef](#)] [[PubMed](#)]
40. Badmaev, B.B.; Dembelova, T.S.; Damdinov, B.B.; Gulgenov, C.Z. Impedance method for measuring shear elasticity of liquids. *Acoust. Phys.* **2017**, *63*, 642–644. [[CrossRef](#)]
41. Dembelova, T.S.; Badmaev, B.B.; Makarova, D.N.; Vershinina, Y.D. Nonlinear viscoelastic properties of nanosuspensions. *IOP Conf. Series Mater. Sci. Eng.* **2019**, *704*, 012005. [[CrossRef](#)]
42. Dembelova, T.S.; Badmaev, B.B.; Makarova, D.N. Investigation of physical-mechanical and tribological properties of suspensions of nanoparticles based on polyethylsiloxane liquid. *J. Phys. Conf. Ser.* **2019**, *1281*, 012009. [[CrossRef](#)]
43. Yamada, Y.; Ichii, T.; Utsunomiya, T.; Sugimura, H. Visualizing polymeric liquid/solid interfaces by atomic force microscopy utilizing quartz tuning fork sensors. *Jpn. J. Appl. Phys.* **2020**, *59*, SN1009. [[CrossRef](#)]
44. Su, B.; Zhou, Y.-G.; Wu, H.-H. Influence of mechanical properties of polypropylene/low-density polyethylene nanocomposites. *Nanomater. Nanotechnol.* **2017**, *7*, 1–11. [[CrossRef](#)]
45. Shim, S.E.; Isayev, A.I. Rheology and structure of precipitated silica and poly(dimethyl siloxane) system. *Rheol. Acta* **2003**, *43*, 127–136. [[CrossRef](#)]
46. Boonstra, B.B.; Cochrane, H.; Dännenberg, E.M. Reinforcement of Silicone Rubber by Particulate Silica. *Rubber Chem. Technol.* **1975**, *48*, 558–576. [[CrossRef](#)]

Disclaimer/Publisher's Note: The statements, opinions and data contained in all publications are solely those of the individual author(s) and contributor(s) and not of MDPI and/or the editor(s). MDPI and/or the editor(s) disclaim responsibility for any injury to people or property resulting from any ideas, methods, instructions or products referred to in the content.